



Title	A compound-specific n-alkane ^{13}C and $^{\text{D}}$ approach for assessing source and delivery processes of terrestrial organic matter within a forested watershed in northern Japan
Author(s)	Seki, Osamu; Nakatsuka, Takeshi; Shibata, Hideaki; Kawamura, Kimitaka
Citation	Geochimica et Cosmochimica Acta, 74(2), 599-613 https://doi.org/10.1016/j.gca.2009.10.025
Issue Date	2010-01-15
Doc URL	http://hdl.handle.net/2115/42575
Type	article (author version)
File Information	GCA74-2_599-613.pdf



[Instructions for use](#)

1
2
3 A compound-specific *n*-alkane $\delta^{13}\text{C}$ and δD approach for assessing source and
4 delivery processes of terrestrial organic matter within a forested watershed in
5 northern Japan
6
7
8

9 Osamu Seki^{1*}, Takeshi Nakatsuka^{1,3}, Hideaki Shibata² and Kimitaka Kawamura¹
10
11

12 ¹*Institute of Low Temperature Science, Hokkaido University, N19W8, Kita-ku, Sapporo, 060-0819,*
13 *Japan*
14

15 ²*Field Science Center for Northern Biosphere, Hokkaido University, Nayoro, Hokkaido 096-0071,*
16 *Japan*
17

18 ³*Now at Graduate School of Environmental Studies, Nagoya University, Furo-cho, Chikusa-ku,*
19 *Nagoya 464-8601, Japan*
20
21
22
23
24
25

26 *Corresponding author (e-mail: seki@pop.lowtem.hokudai.ac.jp, phone: +81-11-706-5504
27
28
29

30 **Running head:** $\delta^{13}\text{C}$ and δD of *n*-alkanes in a forested catchment

31 **Index term:** stable carbon isotope, hydrogen isotope, *n*-alkane, riverine organic matter
32

32 Abstract

33 We measured molecular distributions and compound-specific hydrogen (δD) and stable
34 carbon isotopic ratios ($\delta^{13}C$) of mid- and long-chain *n*-alkanes in forest soils, wetland peats
35 and lake sediments within the Dorokawa watershed, Hokkaido, Japan, to better understand
36 sources and processes associate with delivery of terrestrial organic matter into the lake
37 sediments. $\delta^{13}C$ values of odd carbon numbered C_{23} - C_{33} *n*-alkanes ranged from -37.2 to
38 -31.5 ‰, while δD values of these alkanes showed a large degree of variability that ranged
39 from -244 to -180 ‰. Molecular distributions in combination with stable carbon isotopic
40 compositions indicate a large contribution of C3 trees as the main source of *n*-alkanes in
41 forested soils whereas *n*-alkanes in wetland soil are exclusively derived from marsh grass
42 and/or moss. We found that the *n*-alkane δD values are much higher in forest soils than
43 wetland peat. The higher δD values in forest samples could be explained by the enrichment of
44 deuterium in leaf and soil waters due to increased evapotranspiration in the forest or
45 differences in physiology of source plants between wetland and forest. A $\delta^{13}C$ v.s. δD
46 diagram of *n*-alkanes among forest, wetland and lake samples showed that C_{25} - C_{31} *n*-alkanes
47 deposited in lake sediments are mainly derived from tree leaves due to the preferential
48 transport of the forest soil organic matter over the wetland or an increased contribution of
49 atmospheric input of tree leaf wax in the offshore sites. This study demonstrates that
50 compound-specific δD analysis provides a useful approach for better understanding source
51 and transport of terrestrial biomarkers in a C3 plant-dominated catchment.

52

1. Introduction

52
53 Biomarkers have increasingly become common tools in the reconstruction of past
54 environmental conditions. Molecular analyses of terrestrial biomarker lipids extracted from
55 ocean, lake and bog sediments have been used for reconstructions of paleovegetation and
56 associated paleoclimate histories (e.g., Bird et al., 1995; Ficken et al., 1998; Yamada and
57 Ishiwatari, 1999; Nott et al., 2000; Xie et al., 2000; Xie et al., 2004; Huang et al., 2001; Seki
58 et al., 2003; Schefub et al., 2005; Shuman et al., 2006; Zheng et al, 2007; Seki et al., 2009). In
59 particular, *n*-alkanes have been extensively studied for paleoclimatic purposes. This is
60 because mid- (C_{21} - C_{25}) and long-chain (C_{27} - C_{33}) *n*-alkanes, a major component of leaf waxes
61 and typical biomarkers of vascular plants (Eglinton and Hamilton, 1967), are resistant to
62 microbial degradation and have been widely found in natural environments including marine
63 and lacustrine sediments.

64 Molecular distributions and stable carbon isotopic compositions of mid- and long-chain
65 *n*-alkanes provide powerful paleoclimate information of terrestrial vegetation and climate
66 (Pancost and Boot, 2004). For instance, average chain length (ACL) and P_{aq} (% of aquatic
67 plants) of *n*-alkanes can be used as conventional proxies of continental temperature (Hinrichs
68 et al., 1998) and source input of aquatic plant derived *n*-alkanes (Ficken et al., 2000),
69 respectively. The stable carbon isotopic composition ($\delta^{13}C$) of *n*-alkanes has been used to
70 infer the changes in C3/C4 vegetation where distributions are directly related to climatic
71 conditions (e.g., Bird et al., 1995; Yamada and Ishiwatari, 1999; Huang et al., 2001; Bendle et
72 al., 2006; Bendle et al, 2007). Moreover, recently developed techniques for measuring
73 hydrogen isotope compositions (δD) of *n*-alkanes has potential as a more direct proxy of
74 temperature, precipitation, relative humidity and hydrological cycles of the past (e.g., Xie et
75 al., 2000; Liu and Huang, 2005; Shuman et al., 2006; Hou et al., 2006; Jacob et al., 2007; Seki
76 et al, 2009).

77 It is generally thought that terrestrial organic components deposited in coastal and lake
78 sediments near river systems are mainly supplied by river inflows (Goñi, 1997; Goñi et al.,
79 1997) whereas atmospheric transport of terrestrial materials is a more important delivery
80 process to pelagic sediments in open ocean and lake center sediments (e.g., Huang et al.,

81 2000; Kawamura et al., 2003; Huang et al., 2006). Terrestrial plant-derived biomarkers
82 deposited in coastal marine and lacustrine sediments integrate information about terrestrial
83 ecosystems in catchment basin in the past, but transport processes of organic matter during
84 fluvial delivery to the sediments are highly variable depending on their phase, that is,
85 suspended or dissolved forms. Due to a lack of understanding on the delivery and
86 sedimentation process, paleoclimate applicability of terrestrial biomarkers in marine and
87 lacustrine sediments is less developed than marine biomarkers (Pancost and Boot, 2004).
88 Therefore, it is important to understand how fluvial organic materials accumulate in a
89 catchment basin and how climate records are imprinted in sedimentary deposits for better
90 application of terrestrial biomarkers in the paleoenvironmental studies of marine and
91 lacustrine sediments.

92 *n*-Alkanes are often useful for deciphering source and transport information on terrestrial
93 organic matter in watershed and aquatic environments (Jaffé et al., 1995; Prahl et al., 1994;
94 Fernandes and Sicre, 2000; Mead et al., 2005; Seki et al., 2006). Positive correlations
95 ($r^2 > 0.88$) between concentrations of C₂₅-C₃₁ *n*-alkanes and total organic carbon (TOC) have
96 been reported in the sediments of river basins (Prahl et al., 1994; Fernandes and Sicre, 2000),
97 suggesting that terrestrial plant *n*-alkanes are widely representative biomarkers of fluvial
98 organic matter input. Isotopic measurements of organic matter are useful for identifying their
99 sources in natural environments. Because $\delta^{13}\text{C}$ and δD in plants are controlled by independent
100 mechanisms, compound-specific dual isotopic analyses ($\delta^{13}\text{C}$ - δD) can provide better source
101 information on biomarkers than single isotopic analyses (Chikaraishi and Naraoka, 2005;
102 Chikaraishi et al., 2005; Kurill et al., 2006). In this study, we applied for the first time the
103 molecular distributions and compound specific stable carbon and hydrogen isotopic
104 compositions of *n*-alkanes to study the source and transport of terrestrial plant biomarkers in
105 river water system. Here, we discuss the applicability of this combined approach for
106 identifying sources and transport processes of terrestrial plant biomarkers in a small
107 catchment system.

108

109

2. EXPERIMENTAL

110 2.1. Sampling site

111 Hokkaido University's Uryu experimental Forest is located in northern Hokkaido, Japan
112 (about 44°2N, 142°1E; Fig. 1) and is characterized as a cool temperate forest covered with
113 broad- and needle-leaf trees and by many streams, ponds and lakes. The total area of the
114 drainage basin is 3165 ha, total annual rainfall is more than 1000 mm/years and relative
115 humidity is high (> 75 %) throughout the year. This watershed is characterized by the
116 presence of a deep snowpack (about 2 m) for a long period (November to May). Fluvial
117 discharge reaches its maximum in the spring snowmelt season (Ogawa et al., 2006), and the
118 plant-growing season is restricted to a short summer (June to September). A large amount of
119 organic rich particulate material is supplied from the Dorokawa river system to Lake
120 Shumarinai, especially during the snowmelt season. The wetland is a main source of
121 dissolved organic matter (DOM) in stream water and discharge of DOM via streams plays an
122 important role in the carbon cycle of the Dorokawa catchment system (Ogawa et al., 2006).

123 In the downstream of the Dorokawa river (altitude of 284-310 m), there are several types
124 of wetlands while the upstream area is significantly forested (Xiao-niu and Shibata, 2007).
125 Vegetation in the forest area is characterized by a cool-temperate mixture composed of natural
126 hardwood and conifer species, mainly represented by Sakhalin fir (*Abies sachalinensis*),
127 Mongolian oak (*Quercus crispula*), Japanese Manchurian ash (*Fraxinus mandshurica* var.
128 *japonica*), Erman's birch (*Betula ermanii*), painted maple (*Acer mono*) and Amur cork-tree
129 (*Phellodendron amurense*). Deciduous trees dominant at high elevations (the highest at 681
130 m) while conifer-dominated forests are more developed at low elevations. Deciduous trees are
131 also distributed through the riparian zone. The forest understory is exclusively dominated by
132 dwarf bamboo except for some wetland areas and riparian zones. Site D in Fig. 1 is composed
133 of "spruce swamp forests", which contain sparse but pure stands of spruce with dense thickets
134 of dwarf bamboos in the understory. This site represents the most extensive type of wetland in
135 the Dorokawa basin. Sites F and E are typical wetland, mostly covered by grasses, herbs and
136 mosses.

137 Soils and sediments were taken in June and September 2003. Surface soils and soil cores
138 (0-90 cm depth) were collected from three sites in the forested and upland areas (Sites A, B

139 and C) (Fig. 1). Vegetation in all sites is composed of deciduous and coniferous trees.
140 However, deciduous trees dominate over coniferous tree as an overstory at the highest
141 elevation (Site A), while coniferous trees are more important at the mid (Site B) and low
142 elevation sites (Site C). Surface peat and peat cores (0-120cm depth) (Sites D, E and F) were
143 collected in the lowland wetland area of the catchment. Lake surface sediments (0-5 cm
144 depth) were collected in Lake Shumarinai at the mouth of Dorokawa River (Site G) and at
145 sites distal to the river mouth (Sites H and I). Forest soil and wetland peat cores were cut
146 every 10cm except for the Site D peat core, which was cut every 30 cm. All the sample
147 sections were freeze-dried and stored at -20 °C before analyses. River waters were seasonally
148 collected at 7 sites (Fig. 1) in the watershed from July 2003 to October 2004 for hydrogen
149 isotopic analysis.

150

151 **2.2. Separation and determination of *n*-alkanes**

152 Lipid class compounds were extracted from the dry samples (0.5-7.0 g) with
153 dichloromethane/methanol (95:5) using an accelerated solvent extractor (Dionex: ASE 200)
154 three times at 100°C and 1000 psi (about 69 bar) for 5 min each time. The extracts were
155 concentrated and then saponified with 1.0 M potassium hydroxide/methanol. Neutral
156 components were isolated by extraction with *n*-hexane/dichloromethane (10:1). Aliphatic
157 hydrocarbons were separated from other fractions on a silica gel column by eluting with
158 *n*-hexane. Subsequently, the aliphatic hydrocarbon fraction was separated into saturated and
159 unsaturated aliphatic hydrocarbon fractions by silver nitrate-impregnated silica gel (10 wt%)
160 chromatography for compound-specific δD and $\delta^{13}C$ measurements of *n*-alkanes. The
161 saturated fraction was eluted with *n*-hexane, whereas the unsaturated fraction was
162 subsequently eluted with *n*-hexane/dichloromethane (2:1).

163 *n*-Alkanes were analyzed using a HP6890 GC equipped with an on-column injector,
164 CPSIL-5 CB fused silica capillary column (60 m length, 0.32 mm i.d., film thickness 0.25
165 μm) and flame ionization detector (FID). The GC oven temperature was programmed from 50
166 °C to 120 °C at 30 °C/min and then 120 °C to 310 °C at 5 °C/min. Quantification of lipid
167 compounds was achieved by GC/FID using an authentic *n*-alkane mixture as an external

168 standard. Each compound was identified by GC/mass spectrometry based on retention times
169 and mass spectra. A Trace GC equipped with an HP-5MS fused silica capillary column (30 m
170 length, 0.32 mm i.d., film thickness 0.25 μm) interfaced directly to a mass spectrometer was
171 used for indentifying organic compounds. The temperature program for the GC/MS analysis
172 was the same as the GC/FID analysis.

173

174 **2.3. Stable carbon and hydrogen isotope analyses**

175 Compound-specific $\delta^{13}\text{C}$ values of individual *n*-alkanes were determined using a gas
176 chromatography-isotope ratio mass spectrometry (GC-IRMS) system, which consists of a HP
177 6890 GC equipped with a DB-5 fused silica capillary column (30 m \times 0.32 mm i.d., film
178 thickness 0.25 μm) and an on-column injector, a combustion interface (Finnigan GC
179 combustion III), and a Finnigan MAT delta Plus mass spectrometer. The GC oven temperature
180 was programmed from 50 $^{\circ}\text{C}$ to 120 $^{\circ}\text{C}$ at 30 $^{\circ}\text{C min}^{-1}$, then 120 $^{\circ}\text{C}$ to 310 $^{\circ}\text{C}$ at 5 $^{\circ}\text{C min}^{-1}$.
181 The separated compounds from the GC were introduced on-line to the ceramic tube
182 combustion reactor (850 $^{\circ}\text{C}$) that contained thin CuO and Pt wires. The former wire provides
183 oxygen and the latter acts as a catalyst. In duplicate analyses of selected samples, standard
184 deviations for $\delta^{13}\text{C}$ of *n*-alkanes were found to be within 0.5 ‰ (Table 1). $\delta^{13}\text{C}$ values are
185 given in per mil (‰) notation relative to the Peedee Belemnite (PDB). C_{21} *n*-fatty acid methyl
186 ester whose isotopic values were known ($\delta^{13}\text{C} = -26.2$ ‰, $\delta\text{D} = -227$ ‰) was coinjected with
187 the samples as an internal isotopic standard for stable carbon and hydrogen isotopic
188 measurements of *n*-alkanes.

189 Compound-specific δD values of individual long-chain *n*-alkanes were determined using
190 a GC/thermal conversion/IRMS system consisting of a HP 6890 GC connected to a Finnigan
191 MAT delta Plus XL mass spectrometer. Capillary GC column conditions are equivalent to that
192 of compound-specific $\delta^{13}\text{C}$ analysis. Pyrolysis (thermal conversion) of *n*-alkanes to H_2 was
193 achieved at 1450 $^{\circ}\text{C}$ in a microvolume ceramic tube. A laboratory standard containing C_{16} - C_{30}
194 *n*-alkanes, varying in concentration over a six-fold range and varying in δD from -248 to
195 -42 ‰, was analyzed daily. Analytical accuracy of the laboratory standard was within 5 ‰. In
196 duplicate analyses of samples, standard deviations for *n*-alkane δD measurements were within

197 10 ‰ (most samples showed an error within 5 ‰; see Table 1). δD values are given in mil
198 (‰) notation relative to Standard Mean Ocean Water (SMOW).

199 A concern during hydrogen isotopic measurements is that the reaction ($H_2^+ + H_2 \rightarrow H_3^+ +$
200 H) occurs readily in the ion source of the mass spectrometer. H_3 is not resolved from HD^+ by
201 typical IRMS. After correcting for the contribution of H_3^+ to the mass-3 beam (Sessions et al.,
202 2001), the D/H ratios of *n*-alkanes can be calculated by integrating the mass-2 and mass-3
203 signals. The H_3^+ factor was determined by observing changes in the (mass-3)/(mass-2)
204 ion-current ratio since the pressure of H_2 in the ion source chamber was varied by adjustment
205 of the variable-volume inlet.

206 δD of river water was measured using an IsoPrime PyrOH system (GV-instruments), in
207 which H_2O is converted to H_2 gas by the chromium-reduction method at 1050 °C and
208 introduced into an isotopic ratio mass spectrometer together with the He carrier gas. At the
209 beginning of measurements on a given day, two kinds of standard water were analyzed to
210 determine the SMOW/SLAP scale. Each water sample was measured in triplicate and the
211 standard water also analyzed every 10 samples to account for instrument drift of δD values.
212 The analytical precision (1s) in triplicate measurements is about 0.5 ‰.

213
214

3. RESULTS AND DISCUSSION

3.1. Hydrogen isotopic compositions of stream waters

216 Figure 2 shows seasonal changes in δD values of stream waters in Dorokawa catchment
217 sites 1, 4, 6, 10, 13 16 and 20. The seasonal variations in δD values are characterized by a
218 maximum in summer to autumn (August to October) and minimum in spring (April and May)
219 when snow starts to melt (Ogawa et al., 2006). Thus, the spring minimum δD was likely
220 caused by an increased contribution of the melt water, whose δD values are always lower than
221 that of summer precipitation in boreal regions such as Hokkaido (Dansgaard, 1964). However,
222 the variations are rather small at all sites, ranging from -81 ‰ to -72 with an annual mean δD
223 value of -75‰. Isotopic differences among sites are within 5 ‰ throughout the observation
224 period, which is smaller than the range of seasonal variability. This result indicates that

225 spatiotemporal differences in the isotopic composition of environmental water are small
226 (~8 ‰) in the Dorokawa catchment basin.

227

228 **3.2. Concentrations and molecular distributions**

229 Figure 3 shows typical molecular distributions of *n*-alkanes in surface layer samples at
230 each site in Dorokawa catchment and Lake Shumarinai. As evidenced from ACL (ranging
231 from 27.7 to 30.9; Table 1), the main components of the *n*-alkanes are medium- and
232 long-chain *n*-alkanes (from C₂₃ to C₃₃ *n*-alkanes) in all sites. All samples show a strong odd to
233 even carbon number predominance. Carbon preference indices (CPI) of *n*-alkanes (Bray and
234 Evans, 1961) varied between 4.4 and 13.7. These characteristics demonstrate that *n*-alkanes in
235 the soils, peats and sediments are largely originated from vascular higher plants.

236 Concentrations of total *n*-alkanes range from 4.6 to 435.0 μg/g in all samples. In general,
237 concentrations are significantly higher in wetland peats than in the forest soils and lake
238 sediments. Larger amounts of *n*-alkanes in wetland peat probably reflects to greater
239 preservation of organic matter under anoxic conditions compared to the forested soil where
240 microbial degradation of organic matter occurs largely under aerobic conditions.

241 A number of studies have reported that the molecular distributions of *n*-alkanes
242 significantly depend on plant species and the environments where plants grow (Cranwell,
243 1973; Rieley et al., 1991; Ficken et al., 2000; Nott et al., 2000; Baas et al., 2000; Bi et al.,
244 2005; Sachse et al., 2006; Nichols et al., 2006; Rommerskirchen et al., 2006). Previous
245 studies have shown that molecular distributions of *n*-alkanes in non-emergent (submerged and
246 floating) aquatic plants are characterized by a predominance of medium-chain lengths such as
247 C₂₃ and C₂₅, while those of terrestrial plants are dominated by long-chain homologues (>C₂₉)
248 (Ficken et al., 2000). Emergent aquatic plants have *n*-alkane distributions midway between
249 non-emergent and terrestrial plants. Based on modern plant-leaf wax data, Ficken et al. (2000)
250 defined a new proxy; that is, $P_{aq} = (C_{23}+C_{25})/(C_{23}+C_{25}+C_{29}+C_{31})$, which approximates the
251 proportion of submerged and floating aquatic macrophyte inputs relative to emergent and
252 terrestrial plant inputs to lake sediments. It has also been reported that *Sphagnum* species

253 show molecular distributions similar to submerged plants, being characterized by a
254 dominance of C_{23} and/or C_{25} *n*-alkanes (Ficken et al., 1998; Baas et al., 2000; Nott et al. 2000;
255 Nichols et al., 2006). Several studies have reported that *n*-alkane distributions of trees, shrubs,
256 and emergent water plants tend to show large proportions of the C_{27} *n*-alkane (Rieley et al.,
257 1991; Ficken et al., 2000; Bi et al., 2005; Sachse et al., 2006), whereas those of C_3 grasses are
258 generally dominated by the C_{31} *n*-alkane (Cranwell, 1973; Bi et al., 2005; Rommerskirchen et
259 al., 2006).

260 In general, *n*-alkane distributions in all forested soils (Sites A, B and C) are characterized
261 by a peak at C_{29} or C_{31} . P_{aq} and C_{27}/C_{31} ratios in forest soils range from 0.13 to 0.4 and from
262 0.2 to 1.25, respectively. These characteristics are typical of terrestrial tree leaf waxes,
263 suggesting they represent an important source of *n*-alkanes in soils. In contrast, wetland
264 samples (Sites D, E and F) showed variable molecular distributions, being different from
265 forest soil samples. For instance, samples from Sites D and F are characterized by a
266 pronounced C_{31} peak and relatively low C_{27}/C_{31} ratio (0.07-0.28). The low C_{27}/C_{31} ratios at
267 Sites D and F are consistent with the wetland vegetations dominated by C_3 grass (Cranwell,
268 1973; Bi et al., 2005; Rommerskirchen et al., 2006). Molecular distributions at Site E that are
269 remarkably different from the other sites (Fig. 3), are characterized by relatively high P_{aq}
270 values (0.22-0.44) and a bimodal distribution with two peaks at C_{25} and C_{31} , suggesting a
271 significant input of submerged plants or *Sphagnum* species as well as grasses. Given that
272 *Sphagnum* species are one of the main vegetation types in wetland Site E, the C_{23} and C_{25}
273 *n*-alkanes could be derived from *Sphagnum* species. These results suggest that molecular
274 distributions of *n*-alkanes in surface soil samples presented here generally reflect main
275 vegetation types at each site. On the other hand, molecular distributions of *n*-alkanes in lake
276 sediments (Sites G, H and I) are characterized by relatively low ACL values (<29) and high
277 C_{27}/C_{31} ratios (0.87-1.62) compared to other sites. The high C_{27}/C_{31} ratio suggests a greater
278 contribution from tree leaf-derived waxes rather than grasses and aquatic plants.

279 The molecular distributions and concentrations of *n*-alkanes also vary significantly with
280 depth in both forest and wetland samples (Fig. 4). In forested soils, some profiles seem to
281 have a relationship with depth. In particular, remarkable changes with depth are observed in

282 concentrations and the C_{27}/C_{31} ratios of *n*-alkanes that are relatively high in surface soils, but
283 decreased substantially with depth at all sites (Fig. 4a and 4d). CPI and ACL values also show
284 increases with depth at Sites B and C. In contrast to forested soils, concentrations and
285 molecular distributions in wetland samples do not show any increase or decrease with depth
286 except for Site E where CPI, C_{27}/C_{31} and P_{aq} show a decreasing trend with depth.

287 Down core profiles of *n*-alkanes at Sites A-C and E possibly result from alternation of
288 *n*-alkanes during early diagenesis and/or changes in vegetation in the past. In the forest area,
289 the decreases in concentration down the soil profiles are apparently a result of the degradation
290 of *n*-alkanes during early diagenesis. Similar depth profiles have been reported in three types
291 of soil collected from British uplands (Huang et al., 1996). Decreasing ACL and C_{27}/C_{31} with
292 depth is probably largely due to preferential degradation of low molecular weight *n*-alkanes in
293 the soils rather than changes in vegetation in the past. In a study of Scandinavian peat, it has
294 been found that, in parallel with humification, the major *n*-alkane homologue changed from
295 C_{25} and C_{27} to C_{31} , suggesting selective removal of shorter chain *n*-alkanes in the humification
296 process (Lehtonen and Ketola, 1993). In contrast, the down-core profile of molecular
297 distributions in the wetland sites (D and F) largely reflects changes in input of vegetation in
298 the past rather than diagenetic alternation, given the greater preservation potential of organic
299 matter in wetlands due to anoxic conditions. The large amounts of *n*-alkanes at all depths in
300 the wetland cores suggest that, although the wetland area is smaller than the forested area, it
301 represents an important reservoir of *n*-alkanes in the catchment area.

302

303 **3.3. Compound-specific stable carbon and hydrogen isotopic compositions**

304 The stable carbon isotopic signature of terrestrial plants largely depends on carbon
305 fixation pathway, but is also controlled by plant physiology. Bulk C_3 plant tissues have lower
306 isotopic values ($\delta^{13}C \approx -25\text{‰}$ to -28‰) while that of C_4 plants have higher values ($\delta^{13}C \approx$
307 -10‰ to -14‰) (Smith and Epstein, 1971). Concentrations of atmospheric CO_2 , which
308 decreases with elevation, also influence the $\delta^{13}C$ of terrestrial plants. However, since altitude
309 differences among the sampling sites are small (~ 400 m) in this study, the effect is negligible.
310 Studies of numerous plants taken from the local area have shown that the $\delta^{13}C$ of alkyl lipids

311 in C₃ and C₄ plant are generally ~8 ‰ and ~12 ‰ lighter than those of bulk tissues,
 312 respectively (Collister et al., 1994; Chikaraishi and Naraoka, 2003). It has also been reported
 313 that δ¹³C values are lower in C₃ angiosperms (-38 ~ -32 ‰) than in C₃ gymnosperms (-32 ~
 314 -29 ‰) at single sites (Chikaraishi and Naraoka, 2003; Pedentchouk et al., 2008), reflecting a
 315 difference in plant physiology such as stomatal conductance for CO₂ between the two species.

316 The δD values of plant biomolecules primarily reflect the environmental water that the
 317 plants uptake. δD in environmental water depends on climatic conditions (temperature,
 318 evaporation and precipitation) and varies significantly from -300 to 0 ‰ depending on the
 319 global and local hydrological cycles, and thus biomolecules of plants have almost the same
 320 range of δD as meteoric water (Ehleringer and Rundel, 1989). The δD values of plant
 321 biomolecules are secondarily influenced by kinetic isotopic fractionation during biosynthesis.
 322 Because biosynthesis of *n*-alkane discriminates against deuterium relative to hydrogen
 323 (Sternberg et al., 1984; Sessions et al., 1999), *n*-alkanes in aquatic plants show lower δD
 324 values than their host water by 155-160‰ (Sessions et al., 1999; Huang et al., 2004; Sachse et
 325 al., 2004). Hydrogen isotopic fractionation between environmental water and *n*-alkanes
 326 ($\epsilon_{n\text{-alkane/water}}$) is calculated by the following equation: $\epsilon_{n\text{-alkane/water}} = (\delta_{n\text{-alkane}} + 1)/(\delta_{\text{water}} + 1) - 1$.

327 The C₂₃-C₃₃ *n*-alkane δ¹³C values in all sites ranged from -38 to -31 ‰ and most samples
 328 fell in the range expected for C₃ angiosperm leaf wax (Chikaraishi and Naraoka, 2003;
 329 Pedentchouk et al., 2008) (Table 2). This indicates that the main source of long-chain
 330 *n*-alkanes in the soil samples is C₃ angiosperms rather than C₃ gymnosperms. This may
 331 suggest that the *n*-alkane content of angiosperm leaf wax is much greater than that of
 332 gymnosperms.

333 Depth profiles at Site B and C showed that the C₂₅-C₃₁ *n*-alkanes are gradually enriched
 334 in ¹³C with depth by up to 3 ‰ (Fig. 5). A similar phenomenon has been reported in other
 335 soils, in which no changes in vegetation types (C₃ vs C₄) were found in the past (Huang e al.,
 336 1996; Ficken et al., 1998). A 1.3 ‰ change in isotopic enrichment can be explained by recent
 337 depletion of atmospheric δ¹³C due to fossil fuel burning (Keeling et al., 1984). Another 1.7 ‰
 338 may be explained by early diagenesis associated with heterotrophic reworking (Huang e al.,
 339 1996; Ficken et al., 1998; Chikaraishi and Naraoka, 2006) or changed vegetation in the past.

340 On the other hand, $\delta^{13}\text{C}$ enrichment with increasing depth has not been observed in wetland
341 sites. This suggests that $\delta^{13}\text{C}$ variations of peat core sequences largely reflect changes in $\delta^{13}\text{C}$
342 of source plants in the past. Although molecular distributions showed distinct differences
343 between forest and wetland samples, no clear difference was observed in $\delta^{13}\text{C}$ profiles. A
344 one-way analysis of variance (ANOVA) shows there is no significant difference between $\delta^{13}\text{C}$
345 values of $\text{C}_{25}\text{-C}_{33}$ *n*-alkanes in forest and wetland ($P = 0.559$). This indicates that the $\delta^{13}\text{C}$
346 approach is not sensitive enough to differentiate the sources of organic matter in the
347 catchments.

348 The δD values of $\text{C}_{23}\text{-C}_{33}$ *n*-alkanes in the catchment show a wide range from -186 to
349 -245 ‰ and are depleted in deuterium relative to environmental waters (-80 ~ -72 ‰) (Table
350 3 and Fig. 6). The most striking feature of the *n*-alkane δD values is deuterium enrichment in
351 the forest samples (-214 ~ -186 ‰) compared to the wetland samples (-250 ~ -210 ‰). In fact,
352 the one-way ANOVA shows there is a significant difference between δD values of $\text{C}_{25}\text{-C}_{33}$
353 *n*-alkanes in forest and wetland samples ($P = <0.0001$). This indicates that δD analysis can
354 potentially differentiate *n*-alkanes between forest soils and wetland peats. The δD values of
355 $\text{C}_{25}\text{-C}_{31}$ *n*-alkanes in sediment Sites H and I are -204 to -196 ‰ and fall within the range of
356 forest soils. However, the δD values (-219 ~ -214 ‰) in Site G, which is surrounded by
357 wetland, are rather consistent with the wetland samples. In contrast to the $\delta^{13}\text{C}$ profile,
358 enrichment or depletion in deuterium is independent of the *n*-alkane carbon number (Table 3).
359 Similarly, increasing or decreasing trends with depth are not apparent in the δD profile of the
360 *n*-alkanes at soil Site C (Fig. 6).

361 These considerations suggest that early diagenesis does not significantly alter the δD
362 values of *n*-alkanes in the soil and peat. In fact, a strong propensity for *n*-alkane δD values to
363 retain their original isotopic compositions has been suggested by some studies (Yang and
364 Huang 2003; Dawson et al., 2004). For example, Yang and Huang (2003) compared the δD
365 compositions of individual *n*-alkanes in the sediment matrix from compressional leaf fossils
366 in a Miocene (15-20 Ma) paleo-lake deposit. Distinctive δD patterns of leaf fossils and
367 sediments indicate that leaf lipids retain their original isotopic compositions. Comparison of
368 δD values for *n*-alkanes in turbidites (Late Carboniferous to the Late Permian) taken from

369 different climatic locations revealed distinctive latitudinal patterns of δD values with up to
370 70‰ difference between tropical and high latitudinal sites, suggesting that their indigenous
371 δD signatures have been preserved for 260–280 million years (Dawson et al., 2004).

372

373 **3.4. Cause of different δD values of *n*-alkanes between forest and wetland**

374 Environmental waters cannot be a major cause for the large variability of *n*-alkane δD
375 values in the Dorokawa watershed, because regional isotopic variations in river waters are
376 much smaller than the observed differences in the δD values of forest and wetland *n*-alkanes.
377 Although factors controlling lipid δD values in terrestrial plants are not fully understood,
378 possible factors that may control *n*-alkane δD values, based on previous studies, are either (1)
379 differences in δD values of leaf and/or soil waters that reflect micro-climatic gradients or (2)
380 ecological differences of terrestrial plants.

381 It is expected that relative humidity is higher in the wetland than in the forested area and
382 the degree of evaporation at soil and leaf surfaces is larger in the forested area than the
383 wetland, leading to δD enrichment of leaf water in forest plants compared to wetland grasses.
384 This interpretation is supported by the observational results that δD values of terrestrial plant
385 lipids, which are exposed to significant evaporation, are ~ 30 ‰ heavier than that of aquatic
386 plants, which are protected from deuterium enrichment of leaf water (Chikaraishi et al., 2003;
387 Huang et al., 2004; Sachse et al., 2004).

388 In addition to the difference in humidity, differences in plant life form or plant
389 physiology may contribute to the observed isotopic variations. The results of leaf wax
390 *n*-alkane δD measurements from various types of terrestrial plants collected within the same
391 climatic conditions showed a large variability in lipid δD values among plant types
392 (Chikaraishi et al., 2003; Liu et al., 2006; Hou et al., 2007). Interestingly, significant higher
393 δD values for tree leaf wax *n*-alkanes were reported compared to those for grasses and herbs
394 (Liu et al., 2006; Hou et al., 2007). This isotopic difference has been interpreted as a result of
395 the ecological differences of terrestrial plants, probably leading to different degrees of
396 evapotranspiration. Hence, the observed difference in δD between wetland and forest sites
397 may be caused by different plant types (tree vs grass) as suggested by previous studies.

398 Assuming that δD of environmental water is -75‰ in all sites, apparent hydrogen
399 isotopic fractionation between environmental water and *n*-alkanes is -146 to -123‰ in the
400 forest surface soils and -179 to -143‰ in the wetland surface peats. The apparent hydrogen
401 isotopic fractionations in forest samples are lower than the $\epsilon_{\text{water-alkane}}$ (160‰) between
402 *n*-alkanes and algae uptake water (Huang et al., 2004; Sachse et al., 2006). This suggests that
403 there exists an enrichment of environmental water δD by $15\sim 40\text{‰}$ due to the
404 evapotranspiration at the interface between air and soil or plant leaf, or there is smaller
405 biosynthetic fractionation in forest trees than wetland grasses. On the other hand, relatively
406 high apparent hydrogen isotopic fractionations in the wetland peat suggest that no or less
407 isotopic enrichment ($<15\text{‰}$) exists under high relative humidity condition in wetlands or
408 larger biosynthetic fractionation occurs in wetland plants.

409

410 **3.5. Delivery processes and sources of sedimentary organic matter in Lake Shumarinai**

411 In order to infer sources of *n*-alkanes in lacustrine sediments, we compared molecular
412 distributions of the forest and wetland soils to those of lacustrine sediments. Figure 7 displays
413 a P_{aq} v.s. C_{27}/C_{31} diagram for all the samples studied. In the diagram, the sediment Site G is
414 plot in the same area as forest soil *n*-alkanes (Sites A and C), implying a greater contribution
415 of forest soil derived *n*-alkanes to the sediments. However, the location of Sites H and I in the
416 P_{aq} v.s. C_{27}/C_{31} diagram apparently deviates from all the forest and wetland samples. This
417 deviation may be ascribed to a limited number of soil samples in the Dokokawa catchment. In
418 general, the chemical composition of soils is heterogeneous. Hence our dataset may be
419 insufficient to capture all of the potential soil inputs from the catchment to the lake and
420 suggests the existence of a significant soil reservoir with higher C_{27}/C_{31} values somewhere in
421 the catchment.

422 To further assess the sources of sedimentary *n*-alkanes, we plot $\delta^{13}\text{C}$ and δD values of
423 $C_{25}\text{-}C_{31}$ odd *n*-alkanes (Fig. 8). Based on the $\delta^{13}\text{C}$ v.s. δD diagram, we can discriminate the
424 sources of individual *n*-alkanes in the lake sediments. In contrast to the molecular distribution
425 approach, hydrogen isotopic analyses allows source discrimination. All the *n*-alkanes from
426 Sites H and I plot in the same area as forest soil *n*-alkanes (Sites A to C) while *n*-alkane from

427 sedimentary Site G is plot in the group of wetland Sites D to F or on the mixing line between
428 forest and wetland. Thus, based on the $\delta^{13}\text{C}$ v.s. δD diagram, it is suggested that $\text{C}_{25}\text{-C}_{31}$ odd
429 *n*-alkanes in Sites H and I could be mainly derived from upstream forest soils. Sedimentary
430 $\text{C}_{25}\text{-C}_{31}$ odd *n*-alkanes in Site G may be largely contributed from wetland soil in the lower
431 reaches of the Dorokawa stream system or be associated with both forest and wetland inputs.

432 Therefore, considering the result of compound-specific hydrogen isotopic analyses, we
433 speculate that the difference in the molecular distributions between lake sediments is due to
434 limited number of soil samples in the catchment area. In fact, the high $\text{C}_{27}/\text{C}_{31}$ ratio in offshore
435 sediments (Sites H and I) suggests that tree leaf wax is a plausible source, being consistent
436 with the δD values that clearly exhibit an input of forest tree derived *n*-alkanes in offshore
437 sites. The similar molecular distribution of Site G to forested soil samples suggests a possible
438 contribution from several sources to Site G. As shown in Fig. 3, wetland samples show
439 variable molecular distributions and a mixture of sources may yield molecular distribution
440 similar to the forest samples. The discrepancy between the isotopic and molecular distribution
441 approaches highlights the need for compound-specific isotopic analysis to confirm source
442 evaluation of biomarkers, although molecular distributions could be useful as conventional
443 source estimates of organic compounds.

444 Our results suggests that delivery processes for long-chain *n*-alkanes are spatially
445 different along a transect of the sampling sites of lacustrine sediments. What mechanisms
446 could cause such a spatial distribution of *n*-alkane sources in lacustrine sediments? One
447 possible explanation is that hydrodynamic sorting of different source materials during
448 transport (Keil et al., 1994). This mechanism may be invoked in Lake Shumarinai, i.e. the
449 particulate materials transported from forest area to the lake largely consist of fine clay
450 minerals and thus are preferentially transported long distances, while coarse organic particles
451 containing plant debris from the wetland rapidly sink and are deposited in estuaries. A similar
452 process was recognized in the Mississippi River system in North America (Goñi et al., 1997;
453 Goñi et al., 1998). They suggested a preferential transport of fluvial organic matter that
454 originated from grassland soils in the Mississippi River drainage basin to the offshore in the
455 Gulf of Mexico.

456 Alternatively, it is also possible that relatively high C_{27}/C_{31} ratios in offshore sites can be
457 ascribed to a large atmospheric input of tree leaf waxes to local offshore sites (Gagosian and
458 Peltzer, 1986; Kawamura et al., 2003). Because *n*-alkanes are a major component of
459 epicuticular waxes, which cover leaf surfaces, *n*-alkanes in leaf surfaces can easily be ablated
460 by wind and dust. It is generally accepted that plant wax *n*-alkanes can be transported in the
461 atmosphere to offshore regions. In the forested site, it is expected that ablated waxes will
462 accumulate in the air, suggesting atmospheric input may be important in addition to fluvial
463 delivery. However, aerosol samples were not collected in the study area and thus it is difficult
464 to evaluate the importance of organic aerosol input to the lake sediments. In order to further
465 assess the delivery processes of *n*-alkanes deposited in the Lake Shumarinai sediments,
466 further work including the study of leaf waxes and organic aerosols are needed.

467

468

469

5. CONCLUSIONS

470 Multi-proxy approaches including C_{27}/C_{31} and P_{aq} together with the stable carbon and
471 hydrogen isotopic composition of *n*-alkanes were for the first time applied to geochemical
472 samples in the Dorokawa watershed system, northern Japan, to assess sources and delivery
473 process of terrestrial organic matter. Molecular distributions and stable carbon and hydrogen
474 isotopic compositions in soils reflect *in situ* vegetation in Dorokawa drainage basin. Based on
475 the molecular distributions, *n*-alkanes in forest soils are largely suggested to originate from
476 tree leaves while those in wetland soils are mostly derived from wetland grass and moss.
477 Stable carbon isotopic compositions of *n*-alkanes showed greater contributions of C_3
478 angiosperms as a source of *n*-alkanes in soils of the Dorokawa catchment. Hydrogen isotopic
479 compositions of *n*-alkanes discriminate forest- and wetland soil-derived *n*-alkanes, which
480 showed higher and lower values, respectively. A $\delta^{13}C$ vs. δD diagram clearly indicates that
481 C_{25} - C_{31} *n*-alkanes preserved in offshore sediments are largely derived from forest plants rather
482 than wetland vegetation. This study demonstrates that the hydrogen isotopic composition of
483 organic compounds provides a useful tool for inferring their source and delivery processes in
484 a natural catchment system dominated by C_3 plants.

485
486
487
488
489
490
491
492
493
494
495
496
497
498
499
500
501
502
503
504
505
506
507
508
509
510
511
512
513
514
515
516
517
518
519
520
521
522
523
524
525
526
527
528
529
530
531
532
533

ACKNOWLEDGEMENT

This research is in part supported by the 21st-Century Center of Excellence Program funded by Ministry of Education Culture, Sports, Science and Technology. We thank James Bendle and Jeff Seewald for critical comments and corrections on previous versions of this manuscript. We also acknowledge the reviewers for critical comments on previous versions of this manuscript.

REFERENCES

- Baas, M., Pancost, R., van Geel, B. and Sinninghe Damsté, J. S. (2000) A comparative study of lipids in *Sphagnum* species. *Org. Geochem.* **31**, 535–541.
- Bendle, J., Kawamura, K. and Yamazaki, K. (2006) Seasonal changes in stable carbon isotopic composition of *n*-alkanes in the marine aerosols from the western North Pacific: Implications for the source and atmospheric transport *Geochem. Cosmochim. Acta* **70**, 13-26.
- Bendle, J., Kawamura, K., Yamazaki, K., and Niwai, T. (2007) Latitudinal distribution of terrestrial lipid biomarkers and *n*-alkane compound specific stable carbon isotope ratios in the atmosphere over the western Pacific and Southern Ocean. *Geochim. Cosmochim. Acta* **71**, 5934-5955.
- Bi, X., Sheng, G., Liu, X., Li, C. and Fu, J. (2005) Molecular and carbon and hydrogen isotopic composition of *n*-alkanes in plant leaf waxes. *Org. Geochem.* **36**, 1405–1417.
- Bird, M.I., Summons, R.E., Gagan, M.K., Roksandic, Z., Dowling, L., Head, J., Fifield, L.K., Cresswell, R.G. and Johnson, D.P. (1995) Terrestrial vegetation change inferred from *n*-alkane $\delta^{13}\text{C}$ analysis in the marine-environment. *Geochim. Cosmochim. Acta* **59**, 2853–2857.
- Bray E. E. and Evans E. D. (1961) Distribution of *n*-paraffins as a clue to recognition of source beds. *Geochim. Cosmochim. Acta* **36**, 1185-1203.
- Chikaraishi Y. and Naraoka, H. (2003) Compound-Specific δD - $\delta^{13}\text{C}$ analyses of *n*-alkanes extracted from terrestrial and aquatic plants. *Phytochem.* **63**, 361-371, 2004.
- Chikaraishi, Y. and Naraoka, H. (2005) $\delta^{13}\text{C}$ and δD identification of sources of lipid biomarkers in sediments of Lake Haruna (Japan). *Geochim. Cosmochim. Acta* **69**, 3285–3297.
- Chikaraishi, Y., Yamada, Y. and Naraoka, H. (2005) Carbon and hydrogen isotope compositions of sterols from riverine and marine sediments. *Limnol. Oceanogr.* **50**, 1763-1770.
- Chikarasishi, Y. and Naraoka, H. (2006) Carbon and hydrogen isotope variation of plant biomarkers in a plant–soil system. *Chem. Geol.* **231**, 190-202.
- Collister, J.W., Rieley, G., Stern, B., Eglinton, G. and Fry, B. (1994) Compound-specific $\delta^{13}\text{C}$ analyses of leaf lipids from plants with differing carbon dioxide metabolisms. *Org. Geochem.* **21**, 619–627.
- Dansgaard, W. (1964) Stable isotopes in precipitation. *Tellus* **16**, 436-468.
- Cranwell, P.A. (1973) Chain-length distribution of *n*-alkanes from lake sediments in relation to post-glacial environmental change. *Freshwater Biology* **3**, 259-265.
- Dawson, D., Crice, K. and Alexander, R. (2005) Effect of maturation on the indigenous δD signatures of individual hydrocarbons in sediments and crude oils from the Perth Basin (western Austria). *Org. Geochem.* **36**, 95-104.
- Eglinton, G. and Halimton, R.J. (1967) Leaf epicuticular waxes. *Science* **156**, 1322-1334.
- Ehleringer, J.P. and Rundel P.W. (1989) Stable Isotopes in Ecological Research. edited by P. W. Rundel, et a., 120 pp., Springer-Verlag.

- 534 Fernandes, M.A. and Sicre, M.-A. (2000) The importance of terrestrial organic carbon inputs
535 on Kara Sea shelves as revealed by *n*-alkanes, OC and $\delta^{13}\text{C}$ values. *Org. Geochem.* **31**,
536 363–374.
- 537 Ficken, K.J., Barber, K.E. and Eglinton, G. (1998) Lipid biomarker and plant macrofossil
538 stratigraphy of a Scottish montane peat bog over the last two millennia. *Org. Geochem.* **28**,
539 217-237.
- 540 Ficken, K.J., Li, B., Swain, D.L. and Eglinton, G. (2000) An *n*-alkane proxy for the
541 sedimentary inputs of submerged/floating freshwater aquatic macrophytes. *Org. Geochem.*
542 **31**, 745-749.
- 543 Gagosian, R.B. and Peltzer, E.T. (1986) The importance of atmospheric input of terrestrial
544 organic material to deep sea sediments. *Org. Geochem.* **10**, 661–669.
- 545 Goñi, M.A., (1997) Record of terrestrial organic matter composition in Amazon Fan
546 sediments. *Proc. ODP Sci. Res.* **155**, 519– 530.
- 547 Goñi, M.A. Ruttenger, K.C. and Eglinton, T.I. (1997) Source and contribution of terrigenous
548 organic carbon to surface sediments in the Gulf of Mexico. *Nature* **389**, 275-278.
- 549 Goñi, M.A. Ruttenger, K.C. and Eglinton, T.I. (1998) A reassessment of the sources and
550 importance of land-derived organic matter in surface sediments from the Gulf of Mexico.
551 *Geochim. Cosmochim. Acta* **62**, 3055-3075.
- 552 Hinrichs, K.-U., Rinna, J. and Rullkötter, J. (1998) Late Quaternary paleoenvironmental
553 conditions indicated by marine and terrestrial molecular biomarkers in sediments from the
554 Santa Barbara basin. In: Wilson, R.C., Tharp, V.L. (Eds.), Proceedings of the Fourteenth
555 Annual Pacific Climate (PACLIM) Workshop, pp. 125-133.
- 556 Hou, J., Huang, Y., Wang, Y., Shuman, B., Oswald, W.W., Faison, E. and Foster, D.R. (2006)
557 Post glacial climate reconstruction based on compound-specific D/H ratios of fatty acids
558 from Blood Pond, New England. *Geochem. Geophys. Geosys.* **7**, 2005GC001076.
- 559 Hou, J., D'Andrea, W.J., MacDonald, D. and Huang, Y. (2007) Hydrogen isotopic variability
560 in leaf waxes among terrestrial and aquatic plants around Blood Pond, Massachusetts
561 (USA). *Org. Geochem.* **38**, 977–984.
- 562 Huang, Y.S., Bol, R., Harknes, D.D., Ineson, P. and Eglinton, G. (1996) Post-glacial variations
563 in distributions, ^{13}C and ^{14}C contents of aliphatic hydrocarbons and bulk organic matter in
564 three types of British upland soils. *Org. Geochem.* **24**, 273-287.
- 565 Huang, Y.S., Dupont, L., Sarnthein, M., Hayes, J.M. and Eglinton, G. (2000) Mapping of C4
566 plant input from North West Africa into North East Atlantic sediments. *Geochim.*
567 *Cosmochim. Acta* **64**, 3505– 3513.
- 568 Huang, Y.S., Freeman, K.H., Eglinton, T.I. and Street-Perrott, F.A. (2001) Climate change as
569 the dominant control on glacial–interglacial variations in C3 and C4 plant abundance.
570 *Science* **293**, 1647–1651.
- 571 Huang, Y., Shuman, B., Wang Y. and Webb, T. (2004) Hydrogen isotope ratios of individual
572 lipids in lake sediments as novel tracers of climatic and environmental change: a surface
573 sediment test. *J. Paleolimnol.* **31**, 363–375.
- 574 Huang, Y., Shuman, B., Wang, Y., Webb III, T., Grimm, E.C. and Jacobson Jr. G.L. (2006)
575 Climatic and environmental controls on the variation of C3 and C4 plant abundances in
576 central Florida for the past 62,000 years. *Palaeogeogr. Palaeoclimatol. Palaeoecol.* **237**,
577 428-435.
- 578 Jacob, J., Huang, Y., Disnar, J.-R., Sifeddine, A., Boussafir, M., Albuquerque A.L.S. and
579 Turcq, B. (2007) Paleohydrological changes during the last deglaciation in Northern Brazil.
580 *Quat. Sci. Rev.* **26**, 1004-1015.
- 581 Jaffé, R., Wolf, G.A., Cabrera, A.C. and Chitty, H.C. (1995) The biogeochemistry of lipids in
582 rivers of the Orinoco Basin. *Geochim. Cosmochim. Acta* **59**, 4507-4522.
- 583 Kawamura, K., Ishimura, Y. and Yamazaki, K. (2003) Four year observations of terrestrial

- 584 lipid class compounds in marine aerosols from the western North Pacific. *Global*
 585 *Biogeochem. Cycles* **17**, doi:10.1029/2001GB001810.
- 586 Keeling C.D., Carter A.F. and Mook W. G. (1984) Seasonal, latitudinal, and secular
 587 variations in the abundance and isotopic ratios of atmospheric CO₂. 2. Results from
 588 oceanographic cruises in the tropical Pacific Ocean. *J. Geophys. Res.* **89**, 4615-4628.
- 589 Keil, R.G., Tsamakis, E., Bor Fuh, C., Giddings, J.C. and Hedges, J.I. (1994) Mineralogical
 590 and textural controls on the organic composition of coastal marine sediments:
 591 hydrodynamic separation using SPLITT-fractionation. *Geochim. Cosmochim. Acta* **58**,
 592 879-893.
- 593 Kurill, E., Sachse, D., Mügler, I., Thiele, A. and Gleixner, G. (2006) Compound-specific $\delta^{13}\text{C}$
 594 and $\delta^2\text{H}$ analyses of plant and soil organic matter: A preliminary assessment of the effects
 595 of vegetation change on ecosystem hydrology. *Soil Biol. Biochem.* **38**, 3211-3221.
- 596 Lehtonen, K. and Ketola, M. (1993) Solvent-extractable lipids of *Shagnum*, *Carex*, *Bryales*
 597 *and Carex-Bryales* peats: content and compositional features vs. peat humification. *Org.*
 598 *Geochem.* **20**, 363-380.
- 599 Liu, W. and Huang, Y. (2005) Compound specific D/H ratios and molecular distributions of
 600 higher plant leaf waxes as novel paleoenvironmental indicators in the Chinese Loess
 601 Plateau. *Org. Geochem.* **36**, 851-860.
- 602 Liu, W., Yang, H. and Li, L. (2006) Hydrogen isotopic compositions of *n*-alkanes from
 603 terrestrial plants correlate with their ecological life forms. *Oecologia* **150**, 330-338.
- 604 Mead, R., Xu, Y., Chong, J. and Jaffé, R. (2005) Sedimentary and soil organic matter source
 605 assessment as revealed by the molecular distribution and carbon isotopic composition of
 606 *n*-alkanes. *Org. Geochem.* **36**, 363-370.
- 607 Nichols, J.E., Booth, R.K. and Jackson, S.T. (2006) Paleohydrologic reconstruction based on
 608 *n*-alkane distributions in ombrotrophic peat. *Org. Geochem.* **37**, 1505-1513.
- 609 Nott, C.J., Xie, S., Avsejs, L.A., Maddy, D., Chambers, F.M. and Evershed, R.P. (2000)
 610 *n*-Alkane distributions in ombrotrophic mires as indicators of vegetation change related to
 611 climatic variations. *Org. Geochem.* **31**, 231-235.
- 612 Ogawa, A., Shibata, H., Suzuki, K., Mitchell, M.J. and Ikegami, Y. (2006) Relationship of
 613 topography to surface water chemistry with particular focus on nitrogen and organic
 614 carbon solutes within a forested watershed in Hokkaido, Japan. *Hydrolog. Proces.* **20**,
 615 251-265.
- 616 Pancost, R.D. and Boot, C.S. (2004) The palaeoclimatic utility of terrestrial biomarkers in
 617 marine sediments. *Mar. Chem.* **92**, 239- 261.
- 618 Prah, F.G., Ertel, J.R., Goni, M.A., Sparrow, M.A. and Eversmeyer, B. (1994) Terrestrial
 619 organic carbon contribution to sediments on the Washington margin. *Geochim.*
 620 *Cosmochim. Acta* **58**, 3035-3048.
- 621 Pedentchouk, N., Sumner, W., Tipple, B. and Pagani, M. (2008) $\delta^{13}\text{C}$ and δD compositions of
 622 *n*-alkanes from modern angiosperms and conifers: An experimental set up in central
 623 Washington State, USA. *Org. Geochem.* **39**, 1066-1071.
- 624 Rieley, G., Collier, R.J., Jones, D.M., Eglinton, G., Eakin, P.A. and Fallick, A.E. (1991)
 625 Sources of sedimentary lipids deduced from stable carbon-isotope analyses of individual
 626 compounds. *Nature* **352**, 425-427.
- 627 Rommerskirchen, F., Plader, A., Eglinton, G., Chikaraishi, Y. and Rullkötter, J. (2006)
 628 Chemotaxonomic significance of distribution and stable isotopic composition of
 629 long-chain alkanes and alkan-1-ols in C₄ grass waxes. *Org. Geochem.* **37**, 1303-1332.
- 630 Sachse, D., Radke, J. and Gleixner, G. (2004) Hydrogen isotope ratios of recent lacustrine
 631 sedimentary *n*-alkanes record modern climate variability. *Geochim. Cosmochim. Acta* **68**,
 632 4877-4889.
- 633 Sachse, D., Radke, J. and Gleixner, G. (2006) δD values of individual *n*-alkanes from

- 634 terrestrial plants along a climatic gradient – Implications for the sedimentary biomarker
635 record. *Org. Geochem.* **37**, 469-483.
- 636 Schefub, E., Schouten, S. and Schneider, R.R. (2005) Climatic controls on central African
637 hydrology during the past 20,000 years. *Nature* **437**, 1003-1006.
- 638 Seki, O., Kawamura, K., Nakatsuka, T., Ohnishi, K., Ikehara, M. and Wakatsuchi, M. (2003)
639 Sediment core profiles of long-chain *n*-alkanes in the Sea of Okhotsk: Enhanced transport
640 of terrestrial organic matter from the last deglaciation to the early Holocene. *Geophys. Res.*
641 *Lett.* **30**, 2001GL014464.
- 642 Seki, O., Yoshikawa, C., Nakatsuka, T., Kawamura, K. and Wakatsuchi, M. (2006) Fluxes,
643 source and transport of organic matter in the western Sea of Okhotsk: Stable carbon
644 isotopic ratios of *n*-alkanes and total organic carbon. *Deep-Sea Res. I* **53**, 253–270.
- 645 Seki, O., Meyers, P.A., Kawamura, K., Zheng, Y. and Zhou, W. (2009) Hydrogen isotopic
646 ratios of plant-wax *n*-alkanes in a peat bog deposited in northeast China during the last 16
647 kyr. *Org. Geochem.* **40**, 671-677.
- 648 Sessions, A. L., Burgoyne, T. W., Schimmelmann, A. and Hayes, J.M. (1999) Fractionation of
649 hydrogen isotope in lipid biosynthesis. *Org. Geochem.* **30**, 1193-1200.
- 650 Sessions, A.L. Burgoyne, T.W., Schimmelmann, A. and Hayes, J.M. (2001) Corrections of H₃⁺
651 contributions in hydrogen isotope ratio monitoring mass spectrometry. *Anal. Chem.* **73**,
652 192-199.
- 653 Shuman, B., Huang, Y. and Newby, P. (2006) Compound-specific isotopic analyses track
654 changes in seasonal precipitation regimes in the Northeastern United States. *Quat. Sci. Rev.*
655 **25**, 2992-3002.
- 656 Smith, B.N. and Epstein S. (1971) Two categories of ¹³C/¹²C ratios for higher plants. *Plant*
657 *Physiol.* **47**, 380-384.
- 658 Sternberg, L., Deniro, M.J. and Ajie H. (1984) Hydrogen isotope ratios of saponifiable lipids
659 and cellulose nitrate from CAM, C3 and C4 plants. *Phytochem.* **23**, 2475-2477.
- 660 Xie, S., Nott, C. J., Avsejs, L. A., Volders, F., Maddy, D., Chambers, F. M., Gledhill, A., Carter,
661 J. F. and Evershed, R. P. (2000) Paleoclimate records in compound-specific δD values of
662 a lipid biomarker in ombrotrophic peat. *Org. Geochem.* **31**, 1053-1057.
- 663 Xie, S., Nott, C. J., Avseis, L. A., Maddy, D., Chambers, F. M. and Evershed, R.P. (2004)
664 Molecular and isotopic stratigraphy in an ombrotrophic mire of paleoclimate
665 reconstruction. *Geochem. Cosmochim. Acta* **68**, 2849-2862.
- 666 Xiao-niu, Z. and Shibata, H. (2007) Landscape patterns of overstory litterfall and related
667 nutrient fluxes in a cool-temperate forest watershed in northern Hokkaido, Japan. *J. Forest.*
668 *Res.* **18**, 249-254.
- 669 Yamada, K. and Ishiwatari, R. (1999) Carbon isotopic compositions of long-chain *n*-alkanes
670 in the Japan Sea sediments: implications for paleoenvironmental changes over the past 85
671 kyr. *Org. Geochem.* **30**, 367-377.
- 672 Yang, H. and Huang, Y. (2003) Preservation of lipid hydrogen isotope ratios in Miocene
673 lacustrine sediments and plant fossils at Clarkia, northern Idaho, USA. *Org. Geochem.* **34**,
674 413-423.
- 675 Zheng, Y., Zhou, W., Meyers, P.A. and Xie, S. (2007) Lipid biomarkers in the
676 Zoige-Hongyuan peat deposit: Indicators of Holocene climate changes in West China. *Org.*
677 *Geochem.* **38**, 1927-1940.
- 678

Table 1 Concentration and molecular distribution of *n*-alkanes in Dorokawa catchment

Site	Depth (cm)	Molecular distribution				
		Conc. ($\mu\text{g/g}$)	CPI ^a	ACL ^b	C ₂₇ /C ₃₁ ^c	P _{aq} ^d
Site A-1 (forest)	0-5 cm	28.8	6.2	29.1	0.68	0.22
Site A-2 (forest)	0-5 cm	50.7	8.5	29.9	0.53	0.14
Site A-3 (forest)	0-10 cm	173.5	9.8	29.7	0.55	0.14
Site A-3 (forest)	10-20 cm	24.1	5.9	30.3	0.62	0.21
Site A-3 (forest)	20-30 cm	7.0	5.5	29.2	0.70	0.23
Site A-3 (forest)	50-60 cm	7.5	5.0	28.8	0.35	0.24
Site A-3 (forest)	80-90 cm	0.5	7.0	29.5	0.40	0.19
Site B-1 (forest)	0-5 cm	23.7	6.1	28.7	0.96	0.19
Site B-2 (forest)	0-5 cm	28.4	5.7	30.8	0.20	0.13
Site B-3 (forest)	0-10 cm	20.1	5.7	28.8	0.96	0.24
Site B-3 (forest)	40-50 cm	5.4	6.2	28.9	0.62	0.20
Site B-3 (forest)	80-90 cm	8.4	8.4	28.9	0.59	0.22
Site C-1 (forest)	0-5 cm	21.5	4.4	28.3	1.25	0.35
Site C-2 (forest)	0-5 cm	30.4	6.5	28.4	0.90	0.23
Site C-3 (forest)	0-10 cm	25.1	5.1	27.7	1.18	0.40
Site C-3 (forest)	10-20 cm	22.9	4.7	28.7	0.96	0.22
Site C-3 (forest)	20-30 cm	12.7	4.8	28.6	0.91	0.22
Site C-3 (forest)	30-40 cm	4.1	5.0	28.4	0.91	0.27
Site C-3 (forest)	40-50 cm	7.0	6.7	28.6	0.60	0.27
Site C-3 (forest)	50-60 cm	7.3	7.0	29.1	0.53	0.18
Site C-3 (forest)	60-70 cm	6.5	7.6	29.2	0.48	0.18
Site C-3 (forest)	70-80 cm	4.6	7.7	29.1	0.50	0.19
Site C-3 (forest)	80-90 cm	4.8	8.7	29.3	0.34	0.16
Site D (wetland)	0-30 cm	57.4	6.9	29.9	0.28	0.12
Site D (wetland)	30-60 cm	204.2	8.9	30.5	0.10	0.28
Site D (wetland)	60-90 cm	90.7	8.4	30.3	0.09	0.17
Site D (wetland)	90-120 cm	428.9	7.1	30.1	0.16	0.14
Site D (wetland)	120-150 cm	215.5	5.1	29.8	0.22	0.15
Site E-1 (wetland)	0-10 cm	142.1	6.6	28.1	0.78	0.44
Site E-1 (wetland)	10-20 cm	51.6	6.0	28.4	0.67	0.39
Site E-1 (wetland)	20-30 cm	224.4	6.3	28.5	0.64	0.42
Site E-1 (wetland)	30-40 cm	138.8	5.4	28.1	0.88	0.38
Site E-1 (wetland)	60-70 cm	12.1	4.6	28.4	0.34	0.29
Site E-2 (wetland)	0-10 cm	276.5	7.7	29.7	0.29	0.22
Site E-2 (wetland)	40-50 cm	237.7	6.2	28.6	0.43	0.34
Site F-1 (wetland)	0-10 cm	123.2	7.5	30.0	0.25	0.14
Site F-1 (wetland)	10-20 cm	435.0	8.0	30.9	0.07	0.07
Site F-1 (wetland)	20-30 cm	103.2	7.8	30.2	0.11	0.17
Site F-1 (wetland)	70-80 cm	24.3	6.1	31.7	0.25	0.20
Site F-1 (wetland)	110-120 cm	71.7	7.7	30.8	0.31	0.11
Site F-2 (wetland)	0-10 cm	67.7	8.3	30.6	0.13	0.09
Site G (estuary)	0-5 cm	30.4	7.9	28.8	0.87	0.23
Site H (lake)	0-5 cm	35.8	7.3	28.3	1.34	0.27
Site I (lake)	0-5 cm	10.4	7.4	27.9	1.62	0.31

(a) CPI, carbon preference index, = $2\sum_{\text{odd}} C_{23}\text{-}C_{31}/(\sum_{\text{even}} C_{22}\text{-}C_{34} + \sum_{\text{even}} C_{24}\text{-}C_{36})$.(b) ACL, average chain length, = $(23 * C_{23} + 25 * C_{25} + 27 * C_{27} + 29 * C_{29} + 31 * C_{31} + 33 * C_{33} + 35 * C_{35}) / \sum_{\text{odd}} C_{23}\text{-}C_{35}$.(c) C₂₇/C₃₁, proportion of C₂₇ to C₃₁.(d) P_{aq}, proportion of aquatic plant *n*-alkane, = $(C_{23} + C_{25}) / (C_{23} + C_{25} + C_{29} + C_{31})$.

Table 2 Stable carbon isotopic compositions ($\delta^{13}\text{C}$) of *n*-alkanes in Dorokawa catchment

Site	Depth (cm)	$\delta^{13}\text{C}$ (‰)											
		C ₂₃	S.D. ^a	C ₂₅	S.D. ^a	C ₂₇	S.D. ^a	C ₂₉	S.D. ^a	C ₃₁	S.D. ^a	C ₃₃	S.D. ^a
Site A-1 (forest)	0-5 cm			-33.0	0.5	-32.9	0.2	-34.2	0.3	-33.5	0.1	-35.1	0.2
Site A-2 (forest)	0-5 cm			-33.7	0.3	-33.3	0.1	-34.8	0.3	-34.4	0.0	-37.0	0.2
Site A-3 (forest)	0-5 cm			-32.9		-32.5		-34.0		-34.0		-36.0	
Site B-1 (forest)	0-5 cm			-33.4		-32.0		-33.5		-34.0		-34.5	
Site B-2 (forest)	0-5 cm			-34.9	0.3	-33.5	0.2	-34.6	0.1	-34.4	0.3	-33.5	0.1
Site B-3 (forest)	40-50 cm			-32.1		-32.9		-33.6		-33.1		-33.4	
Site B-3 (forest)	80-90 cm			-32.6		-32.5		-33.1		-33.2		-32.7	
Site C-2 (forest)	0-5 cm			-33.4	0.2	-33.1	0.2	-34.8	0.3	-35.6	0.2	-35.8	0.1
Site C-3 (forest)	10-20 cm			-32.8		-32.8		-35.3		-34.4		-35.6	
Site C-3 (forest)	20-30 cm			-32.6		-32.8		-34.9		-34.4		-35.5	
Site C-3 (forest)	40-50 cm			-31.7	0.2	-32.2	0.3	-33.3	0.3	-33.2	0.1	-34.0	0.4
Site C-3 (forest)	50-60 cm			-31.7		-32.3		-33.5		-33.0		-33.4	
Site C-3 (forest)	70-80 cm			-32.4		-32.3		-32.9		-32.5		-32.8	
Site D (wetland)	0-30 cm	-32.1		-33.0		-34.1		-36.4		-34.5		-34.2	
Site D (wetland)	30-60 cm	-32.7	0.1	-34.8	0.2	-32.2	0.3	-31.3	0.2	-31.5	0.2	-32.1	
Site D (wetland)	60-90 cm	-31.2		-31.7		-32.2		-33.3		-33.2		-34.8	
Site D (wetland)	90-120 cm	-32.0		-32.2		-33.3		-34.7		-33.2		-33.5	
Site D (wetland)	120-150 cm	-32.5	0.1	-32.9	0.0	-37.2	0.5	-35.9	0.5	-34.6	0.1	-34.7	0.4
Site E-1 (wetland)	0-10 cm	-35.2		-34.1		-34.4		-34.2		-34.5		-35.1	
Site E-1 (wetland)	10-20 cm	-34.7		-33.2		-33.5		-33.6		-33.7		-34.6	
Site E-1 (wetland)	20-30 cm	-34.0		-32.8	0.3	-33.2	0.1	-33.5	0.1	-33.9	0.4	-35.1	0.3
Site E-2 (wetland)	0-10 cm	-34.6		-34.3		-34.5		-34.2		-34.4		-35.0	
Site F-1 (wetland)	0-10 cm			-33.3		-32.9		-32.3		-32.3		-32.1	
Site F-1 (wetland)	10-20 cm	-32.6	0.3	-33.6	0.0	-32.1	0.1	-32.4	0.4	-32.6	0.2	-32.6	0.2
Site F-1 (wetland)	20-30 cm			-32.1		-32.7		-32.1		-32.2		-32.1	
Site F-1 (wetland)	110-120 cm	-33.4		-33.6		-33.4		-33.6		-33.7		-35.1	
Site F-2 (wetland)	0-10 cm	-32.6		-33.1		-33.7		-33.8		-33.4		-34.0	
Site G (estuary)	0-5 cm			-32.7	0.1	-32.2	0.3	-32.4	0.2	-32.8	0.2	-32.4	0.1
Site H (lake)	0-5 cm			-32.8		-32.6		-33.1		-33.2		-34.8	
Site I (lake)	0-5 cm	-31.7		-32.7		-33.0		-33.5		-33.7		-34.3	

(a) S.D., standard deviation

Table 3 Stable hydrogen isotopic compositions (δD) of *n*-alkanes in Dorokawa catchment

Site	Depth (cm)	δD (‰)											
		C ₂₃	S.D. ^a	C ₂₅	S.D. ^a	C ₂₇	S.D. ^a	C ₂₉	S.D. ^a	C ₃₁	S.D. ^a	C ₃₃	S.D. ^a
Site A-1 (forest)	0-5 cm			-211	1	-205	0	-203	2	-195	2	-203	1
Site A-2 (forest)	0-5 cm			-211	2	-202	3	-198	5	-194	5	-192	5
Site A-3 (forest)	0-5 cm			-211	1	-201	1	-195	3	-190	1	-204	0
Site B-1 (forest)	0-5 cm			-207	7	-214	4	-211	1	-202	4	-200	6
Site B-2 (forest)	0-5 cm			-210	2	-211	5	-203	2	-199	3	-198	2
Site B-3 (forest)	0-10 cm					-205	4	-212	0	-202	6		
Site B-3 (forest)	40-50 cm			-187	4	-204	8	-208	4	-203	3	-188	2
Site B-3 (forest)	80-90 cm												
Site C-1 (forest)	0-5 cm			-206	2	-208	4	-210	1	-198	0	-187	6
Site C-2 (forest)	0-5 cm			-206	1	-199	3	-195	0	-191	3	-190	9
Site C-3 (forest)	0-10 cm					-192		-213		-190			
Site C-3 (forest)	10-20 cm			-211	4	-214	5	-213	6	-197	4	-191	7
Site C-3 (forest)	20-30 cm			-202	4	-212	0	-214	1	-205	0	-196	2
Site C-3 (forest)	30-40 cm			-199		-198		-203		-191		-193	
Site C-3 (forest)	40-50 cm			-200	9	-197	1	-205	6	-199	1	-188	6
Site C-3 (forest)	50-60 cm			-201		-203		-203		-189		-196	
Site C-3 (forest)	60-70 cm			-203		-203		-186		-180		-197	
Site C-3 (forest)	70-80 cm			-196	5	-200	5	-207	3	-206	0	-186	8
Site C-3 (forest)	80-90 cm			-195	4	-203	4	-199	1	-200	7	-190	13
Site D (wetland)	0-30 cm		5	-214	2	-221	3	-216	0	-229	2	-230	1
Site D (wetland)	30-60 cm		2	-217	5		6	-224	1	-241	2	-232	2
Site D (wetland)	60-90 cm	-228		-221		-223		-208		-202			
Site D (wetland)	90-120 cm			-216	6	-216	1	-218	0	-242	1	-239	2
Site D (wetland)	120-150 cm			-216	5	-227	2	-222	2	-237	2	-236	2
Site E-1 (wetland)	0-10 cm	-227	4	-228	1	-222	1	-217	2	-219	7	-208	5
Site E-1 (wetland)	10-20 cm	-227	0	-233	4	-225	3	-225	7	-220	6	-217	5
Site E-1 (wetland)	20-30 cm	-239	1	-229	1	-220	3	-220	0	-212	1	-211	1
Site E-2 (wetland)	0-10 cm 2	-234	0	-237	4	-223	3	-221	3	-220	3	-222	3
Site E-2 (wetland)	40-50 cm 2	-239	4	-237	5	-221	3	-222	5	-219	3	-224	3
Site F-1 (wetland)	0-10 cm			-212		-210		-227		-240		-230	
Site F-1 (wetland)	10-20 cm					-231	2	-244	0	-240	0	-222	0
Site F-1 (wetland)	20-30 cm					-217	4	-240	1	-243	1		
Site F-1 (wetland)	110-120 cm			-223	2	-211	1	-219	1	-231	3	-219	1
Site F-2 (wetland)	0-10 cm			-231	0	-231	4	-229	1	-241	1	-235	2
Site G (estuary)	0-5 cm	-217	3	-219	1	-217	1	-216	2	-214	2	-213	1
Site H (lake)	0-5 cm			-203	1	-201	6	-202	6	-196	4		5
Site I (lake)	0-5 cm	-207	2	-202	1	-203	1	-204	0	-196	0		

(a) S.D., standard deviation

FIGURE CAPTIONS

682

683

684 Figure 1. Sampling locations in the Dorokawa River watershed and northern part of Lake
685 Shumarinai. Solid circles and triangles represent forest sampling sites (Sites A, B and C) and
686 wetland (Sites D, E and F) soils, respectively. Solid squares represent surface sediment
687 sampling sites in the river and lake (Sites G, H and I). Open circles show river water sampling
688 sites (Sites 1, 4, 6, 10, 13, 16 and 20). Parenthetical numeric numbers indicate the altitude of
689 soil sampling points. The shaded area in the watershed is the wetland area.

690

691 Figure 2. Seasonal changes in hydrogen isotopic compositions of river water (δD_{RW}) in the
692 Dorokawa watershed during the period from July 2003 to October 2004. River water
693 sampling sites are shown in Figure 1.

694

695 Figure 3. Typical molecular distributions of *n*-alkanes in the forest (Sites A-C), wetland (Sites
696 D-F) and lake (Sites G-I) samples in the Dorokawa catchment system and Lake Shumarinai.

697

698 Figure 4. Depth profiles of concentration, carbon preference index (CPI), average chain
699 length (ACL), C_{27}/C_{31} and P_{aq} of *n*-alkanes in forest soils (Sites A-C) and wetland peat (Sites
700 D-F) and lake sediments (Sites G-I). Data for lake surface sediments are represented by
701 shaded vertical bands in the figures.

702

703 Figure 5. Depth profiles of stable carbon isotopic compositions ($\delta^{13}C$) of C_{25} - C_{33} odd carbon
704 number *n*-alkanes in forest (Sites A-C), wetland (Sites D-F) and lake (Sites G-I) samples in
705 the Dorokawa catchment system and Lake Shumarinai. Data in lake surface sediments are
706 represented by shaded vertical bands in the figures. Bars in the figures represent standard
707 deviations.

708

709 Figure 6. Depth profiles of the hydrogen isotopic compositions (δD) of C_{25} - C_{33} odd carbon
710 number *n*-alkanes in forest (Sites A-C), wetland (Sites D-F) and lake (Sites G-I) samples in

711 the Dorokawa catchment system and Lake Shumarinai. Data in lake surface sediments are
712 represented by shaded vertical bands in the figures. Bars in the figures represent standard
713 deviations.

714

715 Figure 7. C_{27}/C_{31} vs. P_{aq} diagrams of *n*-alkanes in the Dorokawa catchment system and Lake
716 Shumarinai.

717

718 Figure 8. $\delta^{13}C$ vs. δD diagrams for odd C_{25} - C_{33} *n*-alkanes in the Dorokawa catchment system
719 and Lake Shumarinai. Bars in the figures represent standard deviations.

Figure 1 (Seki et al.)

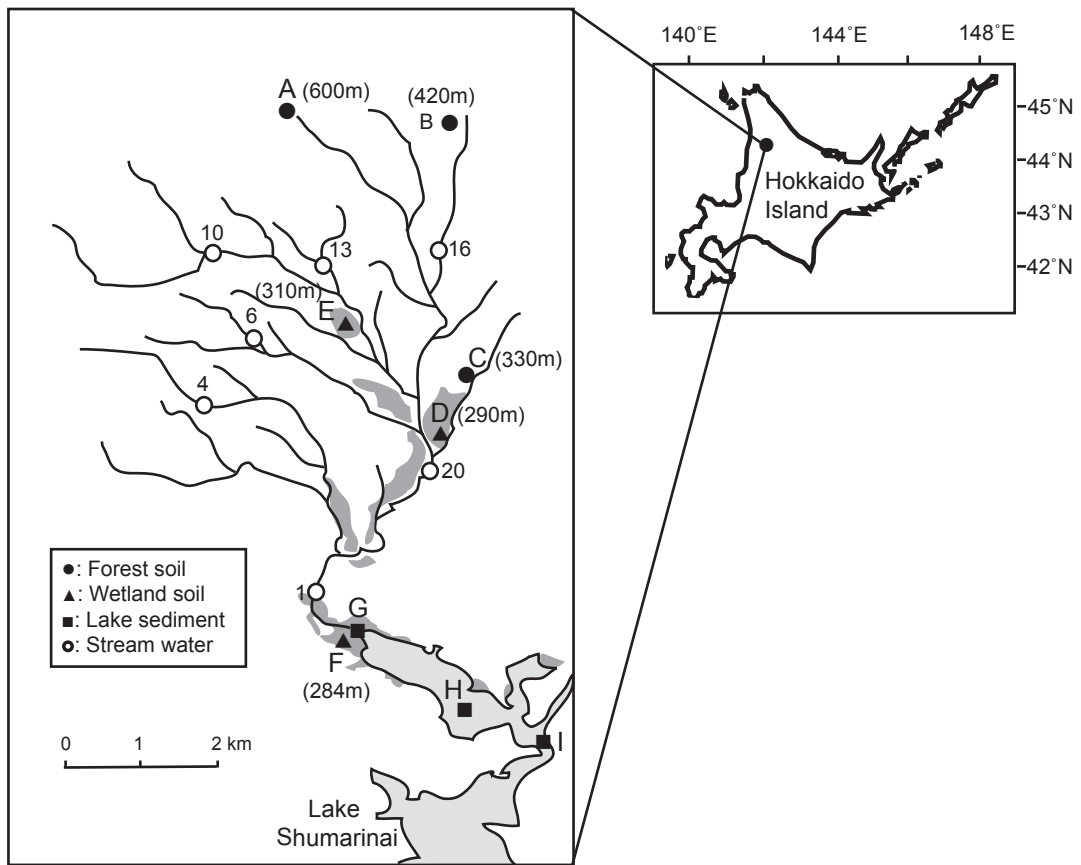


Figure 2 (Seki et al.)

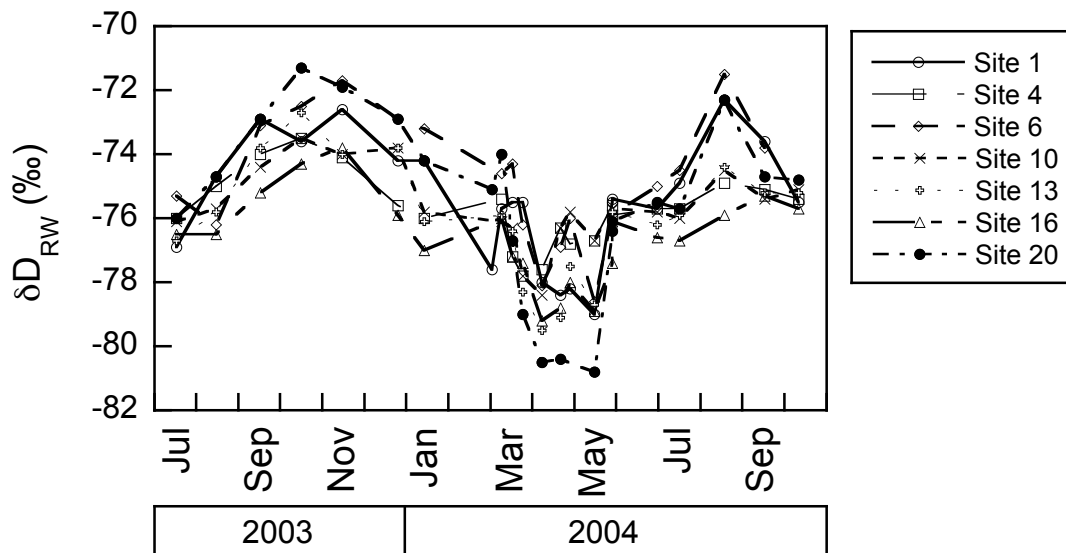


Figure 3 (Seki et al.)

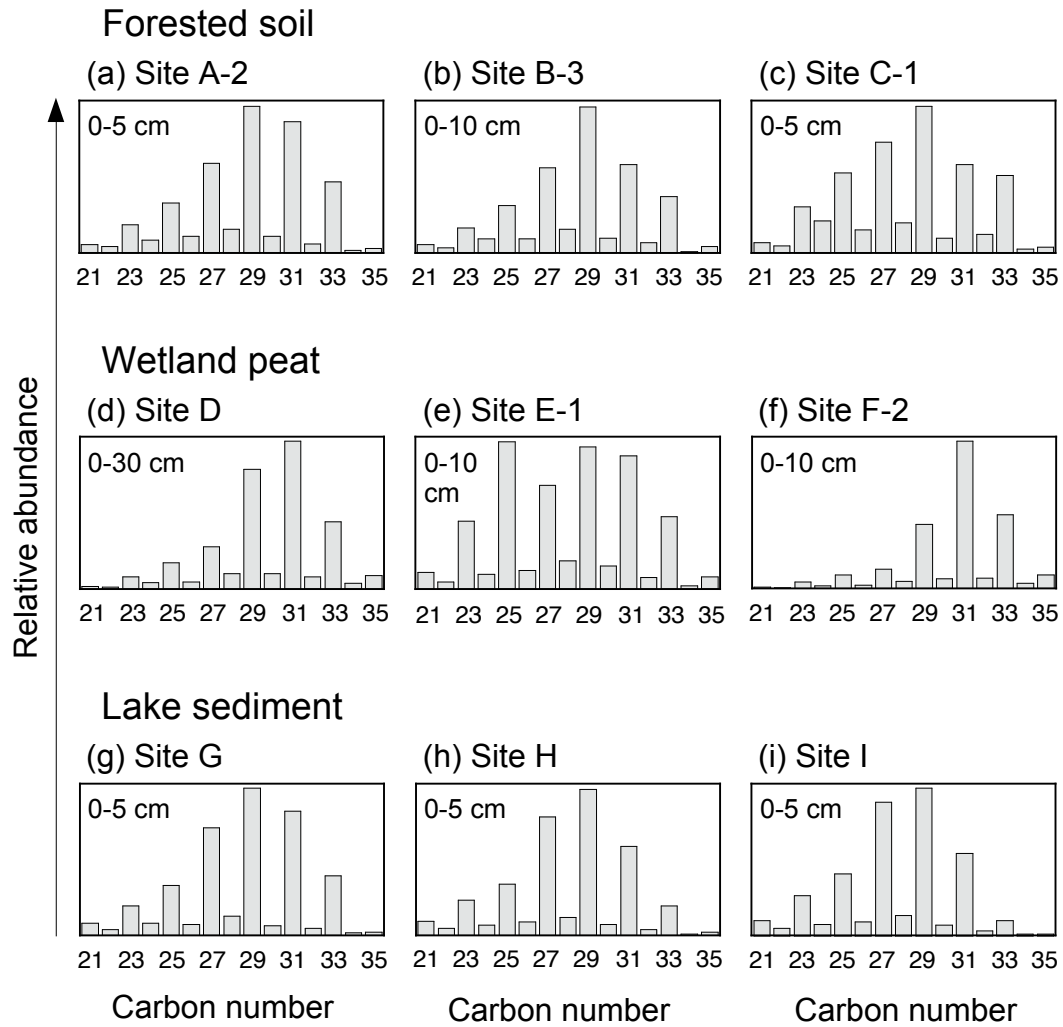


Figure 4 (Seki et al.)

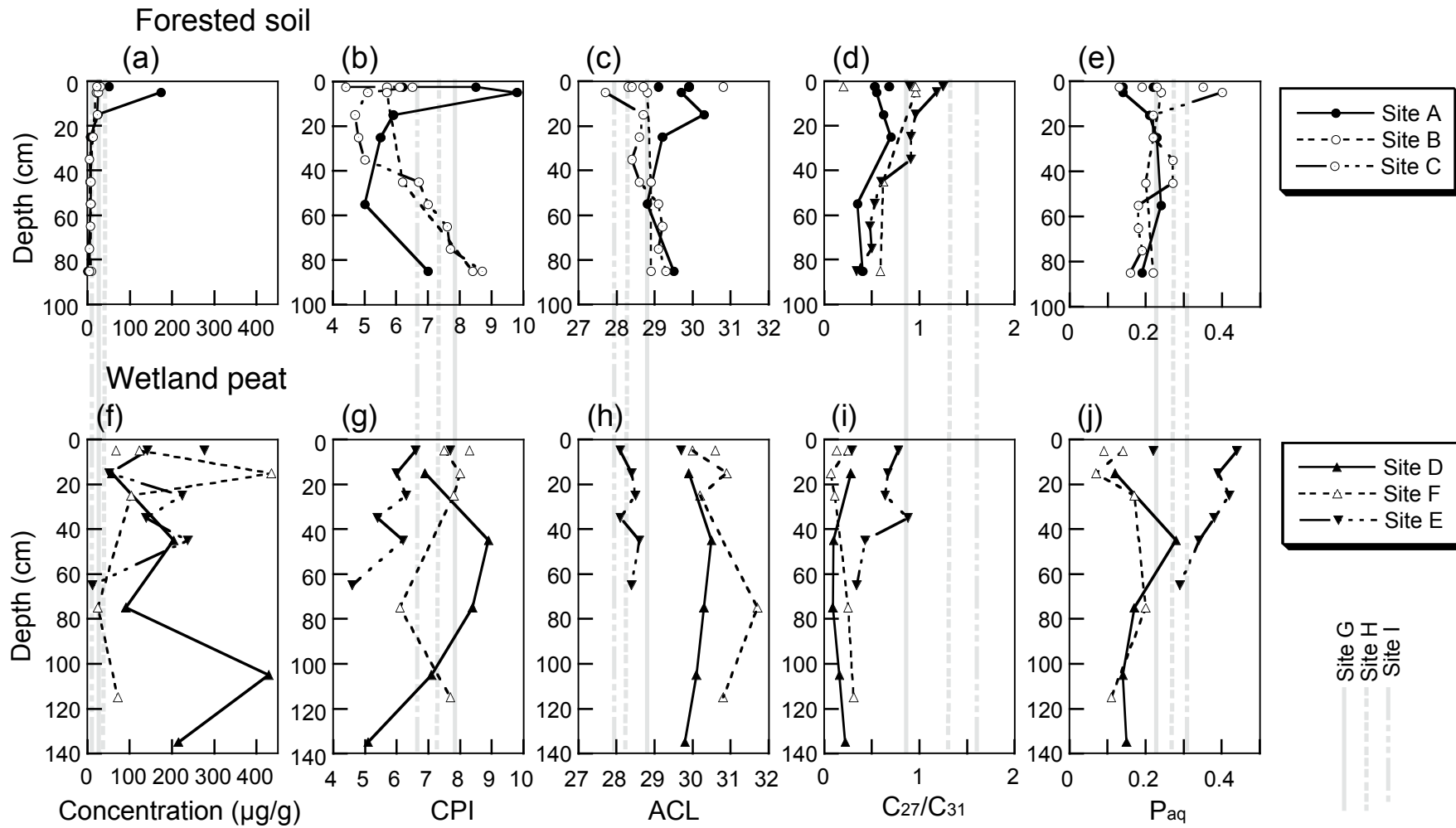
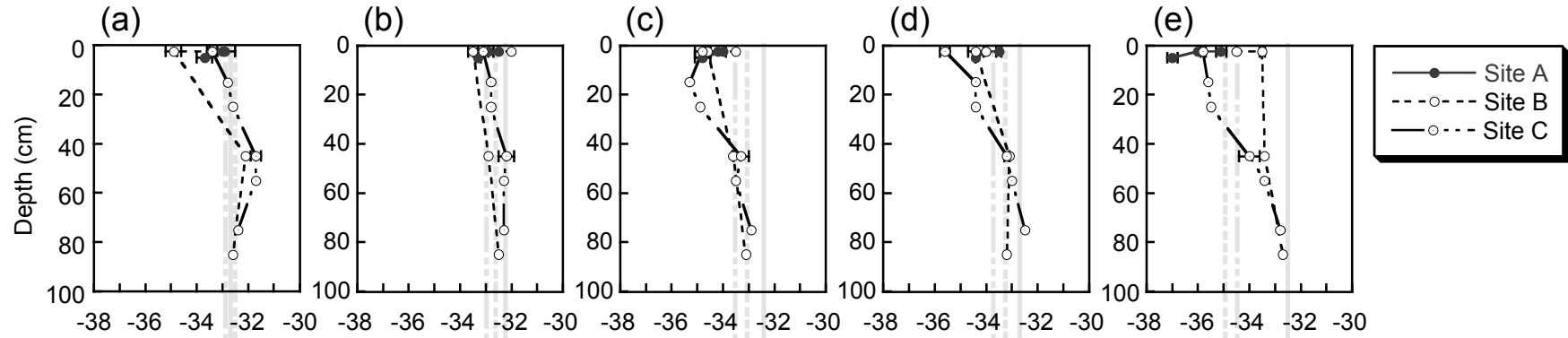


Figure 5 (Seki et al.)

Forested soil



Wetland peat

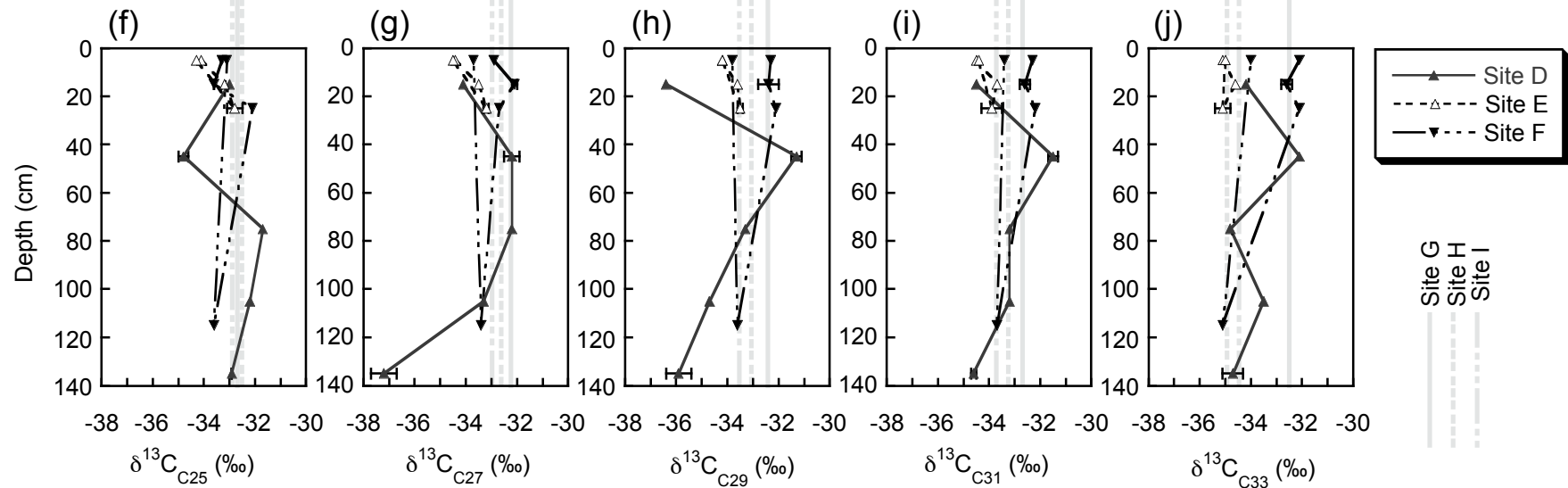
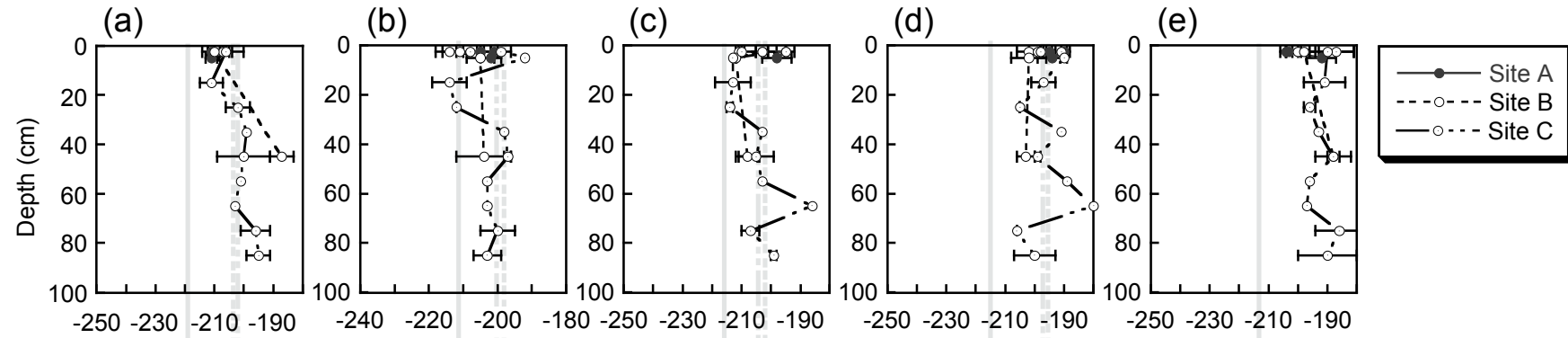


Figure 6 (Seki et al.)

Forested soil



Wetland peat

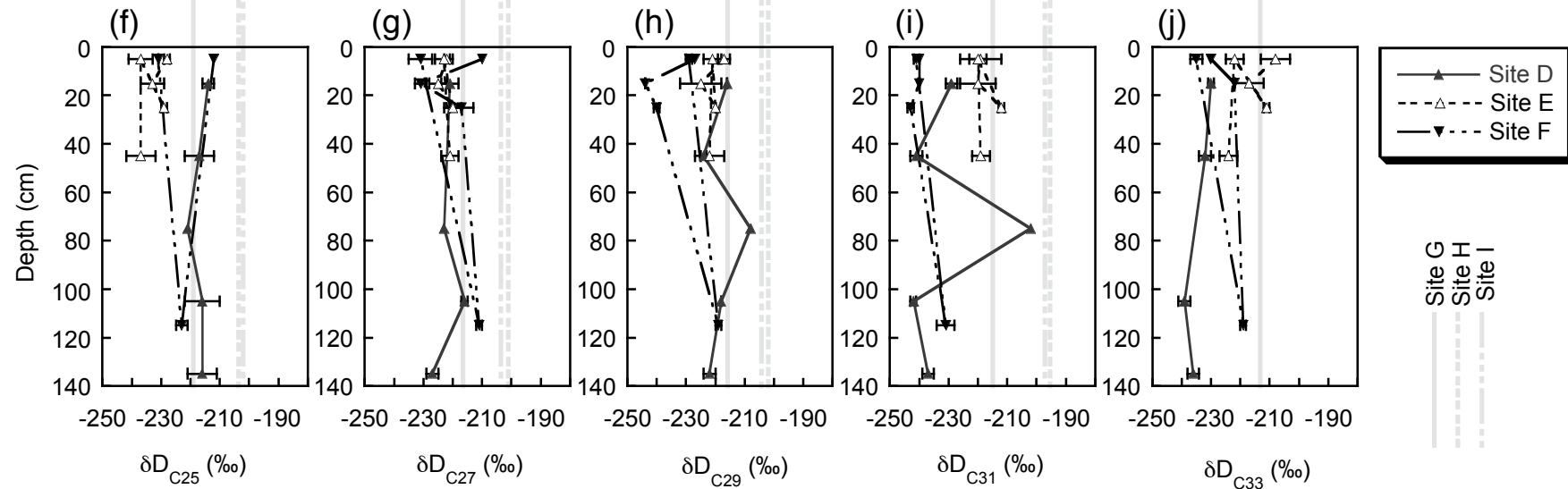


Figure 7 (Seki et al.)

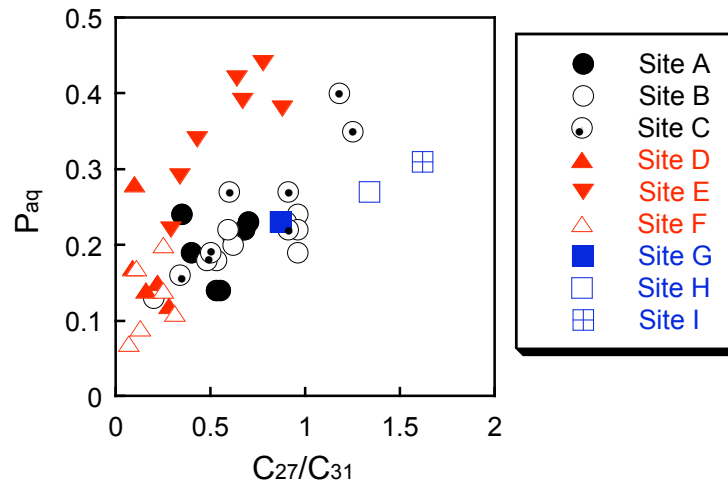


Figure 8 (Seki et al.)

